Golden Standard Technologies:
Inspired by nature. Made by stimOS.

Mimicking Bone Technology
A Golden Standard Technology

Jennifer Knaus[1,2], Dietmar Schaffarczyk*[2], Wolf-Dieter Müller[3], Andreas Schwitalla[3], Helmut Cölfen[1,2] Brigitte von Rechenberg[3]

Comparative Animal Model II:

The impact of surface modifications on PEEK implants based on the covalent bonding of RGD- and KRSR-peptide as well as of hyaluronic acid on the early osseointegration compared to titanium and a hydroxyapatite-filled PEEK

CONFIDENTIAL | PRE-RELEASE | CONFIDENTIAL

Author Affiliations:
1 Department of Chemistry, Physical Chemistry, University of Konstanz, Universitätsstraße 10, 78457 Konstanz, Germany
2 stimOS GmbH, Byk-Gulden-Straße 2, 78467 Konstanz, Germany
3 Charité – Universitätsmedizin Berlin, corporate member of Freie Universität Berlin, Humboldt-Universität zu Berlin and Berlin Institute of Health, Dental Materials and Biomaterial Research, Department of Prosthodontics, Geriatric Dentistry and Craniomandibular Disorders, Aßmannshauser Str. 4-6, 14197 Berlin, Germany
4 Vetsuisse Faculty, Musculoskeletal Research Unit, Competence Center for Applied Biotechnology, University of Zurich, Winterthurerstrasse 204, 8057 Zurich, Switzerland

* corresponding author: Dietmar Schaffarczyk – zyk@stimos.net

NF_2020MBT04

Table of content

Comparative Animal Model II

The impact of surface modifications on PEEK implants based on the covalent bonding of RGD- and KRSR-peptide as well as of hyaluronic acid on the early osseointegration compared to titanium and a hydroxyapatite-filled PEEK

Jennifer Knaus[1,2], Dietmar Schaffarczyk[2], Wolf-Dieter Müller[3], Andreas Schwitalla[3], Helmut Cölfen[1,2] Brigitte von Rechenberg[4]

Author Affiliations:

1 Department of Chemistry, Physical Chemistry, University of Konstanz, Universitätsstraße 10, 78457 Konstanz, Germany
2 stimOS GmbH, Byk-Gulden-Straße 2, 78467 Konstanz, Germany
3 Charité – Universitätsmedizin Berlin, corporate member of Freie Universität Berlin, Humboldt-Universität zu Berlin and Berlin Institute of Health, Dental Materials and Biomaterial Research, Department of Prosthodontics, Geriatric Dentistry and Craniomandibular Disorders, Aßmannshauser Str. 4-6, 14197 Berlin, Germany
4 Vetsuisse Faculty, Musculoskeletal Research Unit, Competence Center for Applied Biotechnology, University of Zurich, Winterthurerstrasse 204, 8057 Zurich, Switzerland

INTRODUCTION

The osseointegration of titanium implants was discovered by chance and described by Brånemark and colleagues in the 1960s [1]. This is characterized by a firm mechanical anchorage of the implant within the bone achieved by bone apposition on the implant surface without connective tissue formation at the bone-implant interface [2]. Accordingly, in the field of dentistry, for example, dental implants in their function as artificial tooth roots enable the firm anchoring of dentures in the jaw [3].

The osseointegration of titanium implants is based on long-term evidence and is made possible by the titanium oxide layer on the implant surface, which due to the strong reactivity of titanium is basically present on the surface of the implant and allows the bone to grow towards it [4]. In general, the largest possible bone-to-implant contact is desired [5].

Nowadays, titanium is also critically evaluated as implant material, suspected to cause problems post-operatively. This is not least due to the fact that titanium can also corrode, particularly in acidic environments [6,7], like in the presence of inflammatory processes [8]. Titanium implants can also corrode in combination with precious metals such as gold for dental application [9]. In principle, the higher the corrosion resistance of a metal, the more biocompatible it is [7]. Corrosion is even more problematic in the presence of intolerance against titanium [10]. This is characterized by the fact that tissue macrophages react with excessive secretion of the inflammation mediators TNF-α and IL-1β [11] after phagocytosis of TiO_2 particles. This leads to osteoclast activation with resulting bone resorption and collagenolysis and thus affecting osseointegration.

In addition, high stresses can occur at the implant-bone interface in dentistry [12,13], which is based on the difference in stiffness between titanium implants and peri-implant bone in combination with the ankylotic anchoring of the implants in the bone and the simultaneous absence of a shock-absorbing periodontal fiber

apparatus as in natural teeth. Titanium has a modulus of elasticity of 110 GPa [13]. Instead for cortical bone the literature gives a modulus of elasticity of 13.8 GPa and for cancellous bone a modulus of elasticity of 1.38 GPa [14]. Based on these facts, there is a risk of overloading the bone, which may lead to its damage and consequently to bone resorption [15-18].

In the fields of orthopaedics and traumatology, the high stiffness of titanium implants in the form of osteosynthesis plates, spinal fusion implants and endoprostheses causes the so-called "stress shielding effect", which leads to an underloading of the neighbouring bone and consequently to its resorption [19,20].
In addition, as in the field of dentistry, there is an increasing desire for metal-free reconstructions [21]. Therefore, implants made of zirconium oxide ceramics have been developed as a metal-free alternative for this area [21]. However, there still seem to be no studies reporting of long-term results that would confirm the use of these implants as a safe form of therapy [22,23]. A disadvantage of this material is that the quality is strongly dependent on the manufacturing process. For example, they may be susceptible to fracture already after manufacture. If instead of the tetragonal phase, which converts into the monoclinic phase to suppress crack propagation within the ceramic, parts of the monoclinic phase are already present on the surface. From there small cracks may then develop [22]. With regard to the theory of overloading the peri-implant bone, it should also be emphasized that zirconium oxide ceramic with a modulus of elasticity of 210 GPa is almost twice as stiff as titanium [24].

For this reason, the high-performance polymer PEEK (polyether ether ketone) is considered an alternative metal-free implant material due to its positive mechanical and biocompatible properties [25]. It has a low density of 1.3 g/cm^3 with a modulus of elasticity of approximately 4 GPa, which can be adjusted by adding (carbon) fibers depending on their degree of filling, length and orientation [25]. For example, a PEEK composite with more than 55 vol-% parallel aligned continuous carbon fibers showed E-moduli in the direction of fiber orientation up to more than 100 GPa [26]. PEEK is frequently used as an implant material in spinal surgery in the form of spine cages [27]. In the field of orthopaedics, the use of PEEK in artificial joints is being researched [28] and in the field of traumatology this material is used as osteosynthesis plates [29]. PEEK implants are also used to reconstruct defects of the bony skull [30] and also interest in dental implants made of PEEK in the field of dentistry was raised [31].

However, a disadvantage of this material is its poor osseointegration potential due to its hydrophobic surface [32]. Accordingly, various surface modification techniques exist to increase the osseointegration of PEEK. Based on the biocompatibility of titanium as an implant material, the surface coating of PEEK implants with titanium is a common procedure [33]. However, such an implant is then not metal-free. Other surface modifications include coating with (nano-) hydroxyapatite (HA) [34] and plasma treatment [35]. However, these showed only slight improvements of osseointegration in animal models. Furthermore, the question arises to what extent a coating with HA remains permanently stable.

Another method is the compounding of PEEK, for example with HA powder [36]. This has the disadvantage, however, that this material can only be processed by milling, as otherwise the incorporated HA particles would not be freely available on the surface and thus the corresponding positive effect on osseointegration would not

occur. Furthermore, it is questionable whether the powder introduced might have a negative effect on the mechanical properties of the PEEK compound. It must also be ensured that the HA powder is homogeneously distributed in the PEEK matrix. However, such a material is commercially available from Invibio Ltd. (PEEK-OPTIMA™ HA Enhanced LT120HAR20, Invibio Ltd., Thornton-Cleveleys, UK), which is said to have improved osseointegrative properties [37].

For the development of a metal-free implant system based on PEEK, a promising method for surface modification seems a covalent binding of certain molecules to the PEEK surface. These molecules are found in proteins of the extracellular matrix (ECM) including bone and serve as binding sites for bone-forming cells. An example is the RGD peptide (amino acid sequence Arg-Gly-Asp), which is found in fibronectin, vitronectin [38] and the family of small integrin-binding ligand N-linked glycoprotein (SIBLING), which includes osteopontin (OPN), bone sialoprotein (BSP (IBSP)), dentin matrix protein 1 (DMP1), dentin sialophosphoprotein (DSPP) and matrix extracellular phosphoglycoprotein (MEPE) [39]. The RGD-motif binds to a large number of cellular transmembrane integrin receptors, whereas the binding to αvβ1 and α5β1 leads to osteogenic differentiation of mesenchymal stem cells (MSC) [40] and promotes cell adhesion and metabolic activity of osteoblasts [41]. In this respect, RGD is ascribed the ability to promote the osseointegration of metallic implants [42]. PEEK with covalently bound RGD coating showed increased cell proliferation, osteogenic differentiation, and bonelike apatite formation in cell culture tests with mouse osteoblasts [43] and promoted the adhesion and proliferation of human osteoblasts [44].

The KRSR peptide (amino acid sequence Lys-Arg-Ser-Arg) is a heparin-binding peptide and acts somewhat more specifically than RGD on bone-forming cells, being present in five bone-related adhesive proteins – also in addition to fibronectin, bone sialoprotein, vitronectin, osteopontin and thrombospondin – and specifically promotes osteoblast adhesion and osteogenic differentiation [45].

Another promising new method for surface modification appears to be the covalent bonding of a thin layer of hyaluronic acid, which is subsequently mineralized with calcium phosphate to mimic calcified ECM of bone [46]. This is a commercial procedure with ISO 13485:2016 certification called "Mimicking Bone Technology" (MBTv, stimOS GmbH, Konstanz, Germany), whereby the "v" in the abbreviation is intended to indicate the use of a hyaluronic acid of vegan (bacterial) origin.

In this respect, the aim of the present study was to assess the osseointegration of PEEK implants to whose surfaces RGD peptide, KRSR peptide and hyaluronic acid were covalently bound compared to implants made of titanium and HA-filled PEEK as control groups in the sheep model.

MATERIAL AND METHODS

Implant manufacture

Initially, a total of 36 cylindrical implants with an external thread (diameter: 3.55 mm, length: 8 mm) were produced by turning from round rods of the following three implant materials:
pure PEEK (i4 R, Evonik Industries, Essen, Germany), for the experimental groups (n=24)
Titanium grade IV (Zapp Precision Metals GmbH, Schwerte, Germany), for the control group 1 (n=6)
PEEK compound filled with 20% HA-powder (PEEK-OPTIMA™ HA Enhanced LT120HAR20(Batch Number: SSR0402), Invibio Ltd., Thornton-Cleveleys, UK), for the control group 2 (n=6).

Subsequently, the 36 experimental implants made of pure PEEK were divided into 4 groups of n=6 implants each according to their respective surface modifications:

RGD: The immobilization of RGD peptide on the PEEK surface was achieved according to the investigation by Becker et al. [44]. In brief, after washing with iso-propanol, the implants were treated with neat ethylene diamine (EDA) for 3 h at 120 °C and rinsed with water and alcohol afterwards. The resulting aminated polymer (PEEK-NH_2) was then reacted with 5% (v/v) diethylene glycol diglycidyl ether (Polysciences, Hirschberg, Germany) in 50 mM carbonate buffer (pH 9) for 2 h. Grafting of the peptide was accomplished by incubating the specimens in 0.2 mg/ml RGD (Sigma Aldrich, Munich, Germany) in carbonate buffer for at least 3 h or overnight, followed by washing with water and alcohol.

KRSR: For the covalent coupling of the KRSR-peptide, another immobilization procedure had to be used, as the first amino acid (lysine, K) was involved in binding, but contains two free amino groups preventing defined conjugation. Thus, the peptide extended with a few amino acids and a C-terminal cysteine was used in combination with the heterobifunctional crosslinker 3-maleimidopropionic acid N-hydroxysuccinimide ester (NHS-Prop-Mal). PEEK-NH_2 (prepared as described above) was reacted with 0.5 mg/ml NHS-Prop-Mal in phosphate buffer saline (PBS, pH 7.4) containing 50% dimethylformamide for 3 h and washed copiously with water. The custom-synthesized and purified to 95 % peptide KRSRGYC (GeneCust, Ellange, Luxemburg) was dissolved in 50 mM carbonate buffer (0.5 mg/ml, pH 9.0) and subsequently reacted with the crosslinker activated material for additional 3 h. Washing was carried out with water and alcohol.

MBTv: This procedure was carried out by stimOS GmbH (Konstanz, Germany),
after cleaning the PEEK implant surfaces in a series of liquid baths and subsequent drying, they were activated by oxygen plasma treatment. Directly after the activation, the implants were dip-coated with a solution containing an azidoaniline functionalized polysaccharide. This modification comprised the coupling of a photoactive azidoanilin-linker onto the -COOH side-chains of the polysaccharide with the help of carbodiimide coupling chemistry. After drying, the PEEK surfaces were illuminated with UV-light, coupling the polysaccharide to the surface. In the next synthesis step, the polysaccharide-layer was mineralized with Calcium phosphate. For this, the PEEK implant surfaces were immersed in a Calcium containing solution. A Phosphate-containing solution was added under controlled conditions to the Calcium-solution: constant addition rate, constant

temperature, constant pH and stirring. After the mineralization was completed, the implants were washed and dried under mild conditions.

Additionally, another group of n=6 implants, which were surface-modified according to **MBTg**, were also installed within the frame of the present animal study. This is also a commercial surface modification with ISO 13485:2016 certification based on gelatin instead of hyaluronic acid and was also carried out by stimOS (Konstanz, Germany). However, the results of these are presented in the first part of this white paper „Bone Mimetic Implant Coating Facilitates Early Osseointegration“ and will be published separately.

Subsequently, all implants were packed in double peel bags and subjected to industrial gamma sterilization using 25-50 kGy radiation.

ANIMALS AND SURGICAL MODEL

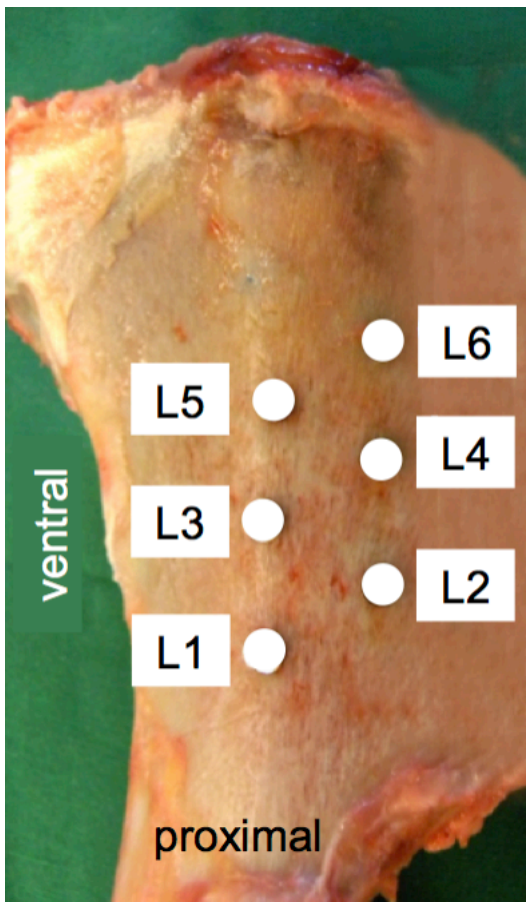

Three adult female Swiss Alpine sheep were used for the experiment. They were born on the same day, 4 years old and their average weight was 91.7 kg (88-98 kg). The animal experiment was carried out according to the Swiss laws of animal protection and welfare (TSchG 455) and were authorized by the local federal authorities (approval no. ZH132/18). The well described and reliable pelvic sheep model was used for the study because of the transferability to humans [47,48]. The implants were installed in the cranial part of the left (n = 6) and right (n = 6) pelvis of each animal (Fig.1), whereas their position alternated on either side of the linea glutea of the iliac bone. The animals were sacrificed 8 weeks postoperatively and the n = 6 implants of each implant group were examined histologically.

Fig.1: Implantation scheme on a left pelvis.

ANAESTHESIA

Sheep were adapted to their new environment 2 weeks prior to surgeries. Sheep were sedated with xylazine (0.1 mg/kg BW Rompun® 2%, Bayer Health Care, Provet AG Lyssach, Switzerland) and buprenorphine (0.01 mg/kg BW Temgesic®, Essex Chemie AG, Luzern, Switzerland). Anesthesia was induced with diazepam (0.1 mg/kg BW Valium®, Roche Pharma AG, Reinach, Switzerland), ketamine (3-5 mg/kg BW Narketan 10®, Vetoquinol AG, Belp-Bern, Switzerland) and propofol (0.2 mg/kg BW 1% MCT Fresenius®, Fresenius Kabi AG, Stans, Switzerland). Anesthesia was maintained with inhalation anesthesia with 1-1.5% isoflurane (Forene®, Abbott AG, Baar, Switzerland) under constant intravenous fluid application (Lactate Ringer 10 ml/kg BW/h) and propofol infusion (1 mg/kg BW/h) using an injection pump and monitoring (pulse oxymetry, capnography, EKG, invasive blood

pressure monitoring). Analgesia was achieved with an additional epidural anesthesia (morphine-HCL 0.1 mg/10 kg BW, Sintetica SA, Mendrisio, Switzerland) at the foramen lumbosacrale during surgery and injection of carprofen (4 mg/kg BW Rimadyl®, Pfizer AG, Zurich, Switzerland) for 4 days. Buprenorphine (0.01 mg/kg BW Temgesic®, Essex Chemie AG, Luzern, Switzerland) was given perioperatively and continued three times in 4 h intervals. Tetanus serum (3000 IE Intervet®, Veterinaria AG, Zurich, Switzerland) and antibiosis (Penicillin Natrium Streuli®, Streuli Pharma AG, Uznach, Switzerland 30,000 IE/kg BW and Gentamycin-Vetagent®, Veterinaria AG, Zurich, Switzerland 4 mg/kg BW) were given prophylactically.

SURGICAL PROCEDURE AND POSTOPERATIVE CARE

Sheep were placed in lateral recumbency with the pelvis slightly inclined toward the surgeon. The surgery was conducted according to the technique described before.

Briefly, access to the pelvis was achieved via a 15- to 20-cm-long slightly curved skin incision in the longitudinal direction of the iliac bone at the mid-pelvis line. The fascia was cut, and the middle gluteal muscle and tensor fasciae latae were carefully separated. The tendinous insertion of the deep and middle gluteal muscles was separated close to the iliac wing in the lower third of the muscle insertions at the iliac crest. For a full exposure and access to the entire iliac wing, Langenbeck retractors were applied. During surgery, a prefabricated bendable template visualized the implantation scheme. Implant sites were prepared according to a standard and approved drilling protocol under cooling with sterile saline solution (0.9 %) using rotating pilot and twist drills made of ceramic (CeraDrill, Gebr. Brasseler GmbH & Co. KG, Lemgo, Germany) completed with adjustable PEEK depth stops in ascending diameter (2.0, 2.8, 3.5 mm). To prepare the apical third of the implant bed a drill with the final diameter of 3.5 mm was customized with a flat drill tip to avoid any major mismatches between the implant and its bed.

Three implants were inserted dorsally and three ventrally to the linea glutea in the right (R) and left (L) pelvis, where position 1 was the most caudal and position 6 the most cranial (Fig.1). Afterwards, the triangle-shaped recess for the insertion tool of the implants was closed with PEEK caps which had a clamping fit. Muscles were repositioned, and the tendinous insertion resutured to its origin with cross sutures. Fascia and subcutis were closed with synthetic resorbable sutures (Polyglactin, Vicryl 2-0, Johnson&Johnson Int., Brussels, Belgium), while the skin was closed with staples (Davis+Geck Appose ULC1, Braun Aesculap AG, Tuttlingen, Germany). Gauze was applied as wound protection before the animal was turned over to the other side. The surgical procedure was repeated in an identical manner on the contralateral pelvis. Postoperatively, sheep were kept in small boxes for 2 weeks and then transferred to larger stalls for the remaining time of the study. After 8 weeks, the sheep were sacrificed.

INTRAVITAL FLUORESCENCE MARKERS

To reveal dynamic calcium deposition over time, fluorescence dyes were applied. These bind to calcium in the blood stream, which is incorporated into newly deposited and mineralized bone matrix 12–72 h after application.

Fluorescence labeling was performed via subcutaneous injections of calcein green (1 ml/kg; Fluka AG, Buchs, Switzerland), xylenol orange (1 ml/kg; Fluka AG) and oxytetracyclin (20 mg/kg KGW s.c., Engemycin® 10%; Intervet ad us. Vet., Veterinaria AG, Freienbach, Schweiz, Switzerland) at 2, 4 and 8 weeks (=72 h before sacrifice) after surgery, respectively.

Fluorescent dyes were detected in histological sections using a fluorescence microscope (LeicaDM6000B, Camera DFC350 FX; Leica Microsystems, Glattbrugg, Switzerland) with the appropriate filters (L5 for calcein green, N3 for xylenol orange and D for oxytetracyclin).

HARVESTING OF THE SPECIMENS

Immediately after sacrifice, the pelvis was harvested and the implants were identified through scraping off partially overgrown periosteal bone from the implant caps. The implants were checked for clinical stability, respectively, loosening. Surrounding tissues were assessed macroscopically for any visible signs of inflammation or other changes. Radiographs (2 views, 55 kV/12 s, 60 kV/12 s) of each iliac wing were taken using a specimen radiography system (Faxitron® LX-60 Cabinet X-ray System, Faxitron X-Ray LLC, Lincolnshire, IL, USA). With a band saw (KOLBE Nirotechnik Maschinenbau, Riniker AG, Rupperswil, Switzerland), the wings of the pelvis were cut into bone blocks, in the middle of which were the implants.

HISTOLOGY

The specimens were then fixed in 40% ethanol at 4°C and further dehydrated in an ascending series of ethanol (50%, 70%, 80%, 90%, 96% and 100%).

Afterwards, they were defatted in xylene under vacuum [49]. Two outer surfaces of the samples were cut parallel to the implant axis to allow serial cuts and an exact splitting of the implants along the long axis after embedding. Specimens were infiltrated with methylmethacrylate (Methacrylic acid methyl ester, Sigma-Aldrich Chemie GmbH, Buchs, Switzerland), dibutyl phthalate (Merck KGaA, Darmstadt, Germany) and perkadox 16 (Dr. Grogg Chemie AG, Stettlen-Deisswil, Switzerland) in the proportion 89.5 : 10 : 0.5 and embedded in the same solution using customized Teflon molds, which were placed in a water bath at 30°C for 7 days. After polymerization, the samples were mounted on plastic frames and cut with a precision diamond band saw (EXAKT 300 CL, EXAKT Advanced Technologies GmbH, Norderstedt, Germany). One section of 400 mm thickness was used for normal bone histology, applying a toluidine blue surface staining. A thinner, native section (150–200 mm) was used for fluorescence microscopy and wrapped in aluminum foil to prevent photobleaching. Both were

ground to ca. 200µm, resp. 50µ before being mounted on acrylic sections for conventional and on glass sections for fluorescence microscopy.

The stained thicker sections were then digitally recorded with a macroscope (Leica M420, Camera DFC 320, Leica Microsystems, Heerbrugg, Switzerland; magnification 0.5 X 8) using a specialized software (Leica, IM 1000 Image manager) for semiquantitative evaluation of the BIC, peri-implant bone remodeling, and the presence of a fibrous encapsulation.

HISTOMORPHOMETRY

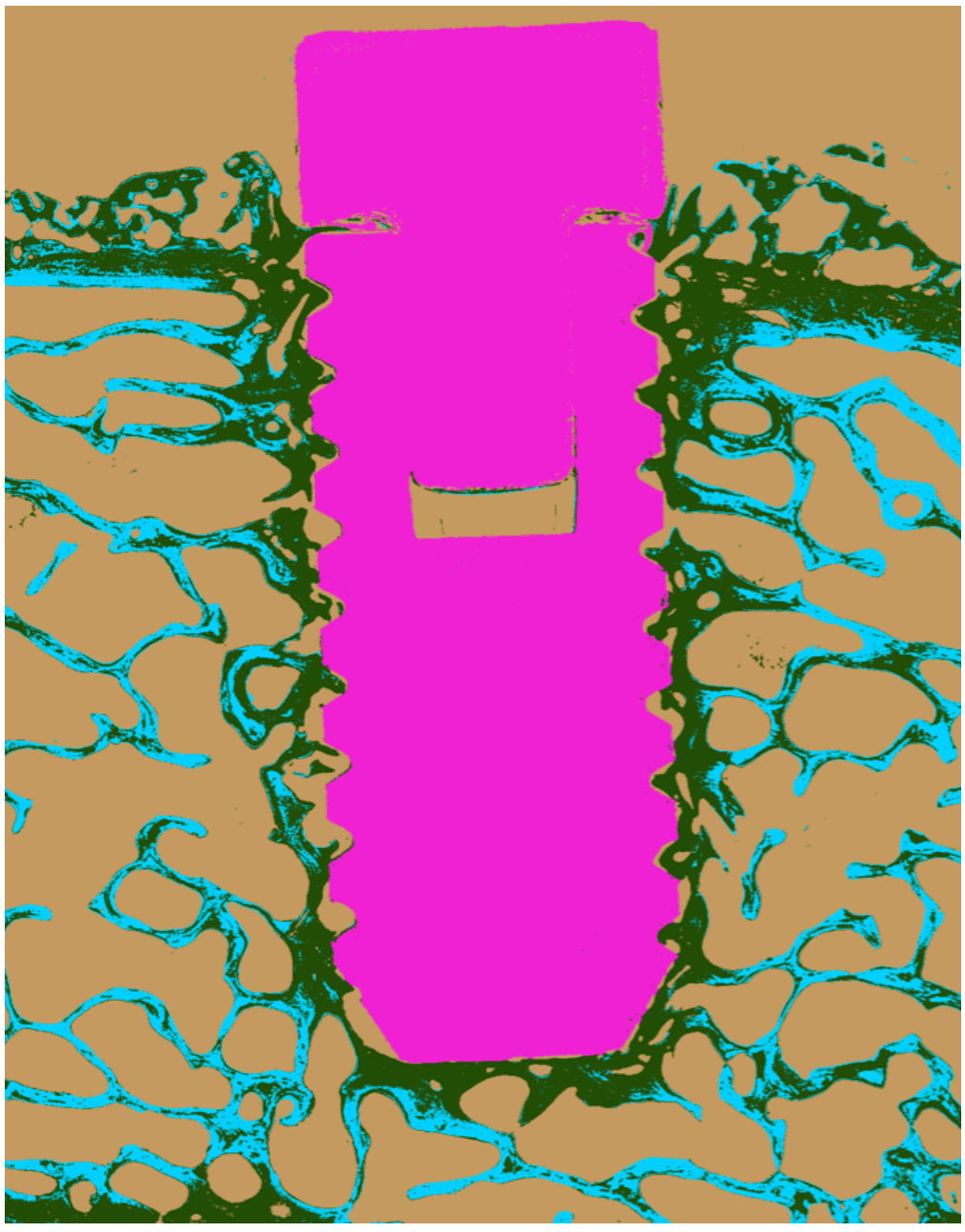

For the evaluation of old and new bone around the implants, zones around the implants in the digitized pictures of the histologic sections were framed using Adobe Photoshop Elements 8 (Adobe Photoshop 3.0) (Adobe Systems, Inc. San Jose, California, United States), such that the area of new bone or fibrous tissue formation could be measured in an area around the implant that corresponded to twice the thread depth. The various tissues were detected manually using the Adobe Photoshop program giving each fraction a different color (new bone = dark green, old bone = turquoise, granulation/ fibrous tissue = light brown; Fig.2). These fractions were then measured with a special analysis software software using a specialized image analysis software program (Fiji, University of Wisconsin) and the colored fractions were automatically detected and measured in number of pixels. Afterwards the pixels within the area of interest (exclusion of background and screw) were set as 100% and the percentage of the different tissues was quantified. Results were exported into a spreadsheet (Excel, Microsoft Office 2010) where the percentage of each fraction/total tissue volume and zone was calculated.

Fig.2: Processed image to evaluate the areas of old and new bone at a titanium implant. The turquoise bone areas around the implant (purple) represent old bone areas and the dark green bone tissue, which are mainly present in the areas closer to the implant, represent newly formed bone.

For the BIC, the percentage of the implant surface in direct contact with mineralized bone was determined by intersection counting within the thread area. Per sample, six thread pitches were counted. The evaluation was performed at calibrated digital pictures at 10-fold magnification (Leica Z6 APOA, Leica DFC 420C, Glattbrugg, Switzerland). Two pictures covered the full threaded part in high resolution.

Then, the length of the total implant surface on both longitudinal surface segments, divided in a cortical and a cancellous portion, was measured using a specialized software offering a tool to follow the lines (Fiji, University of Wisconsin). This was followed by measurement of the actual contact line between bone and implant separately on each side, which was then presented as total BIC or divided in its cortical and cancellous portions. The BIC percentage was then calculated as the portion of implant surface with a direct bone-to-implant connection divided through the total implant surface length (Fig.3). Means of thread counts per implant were calculated

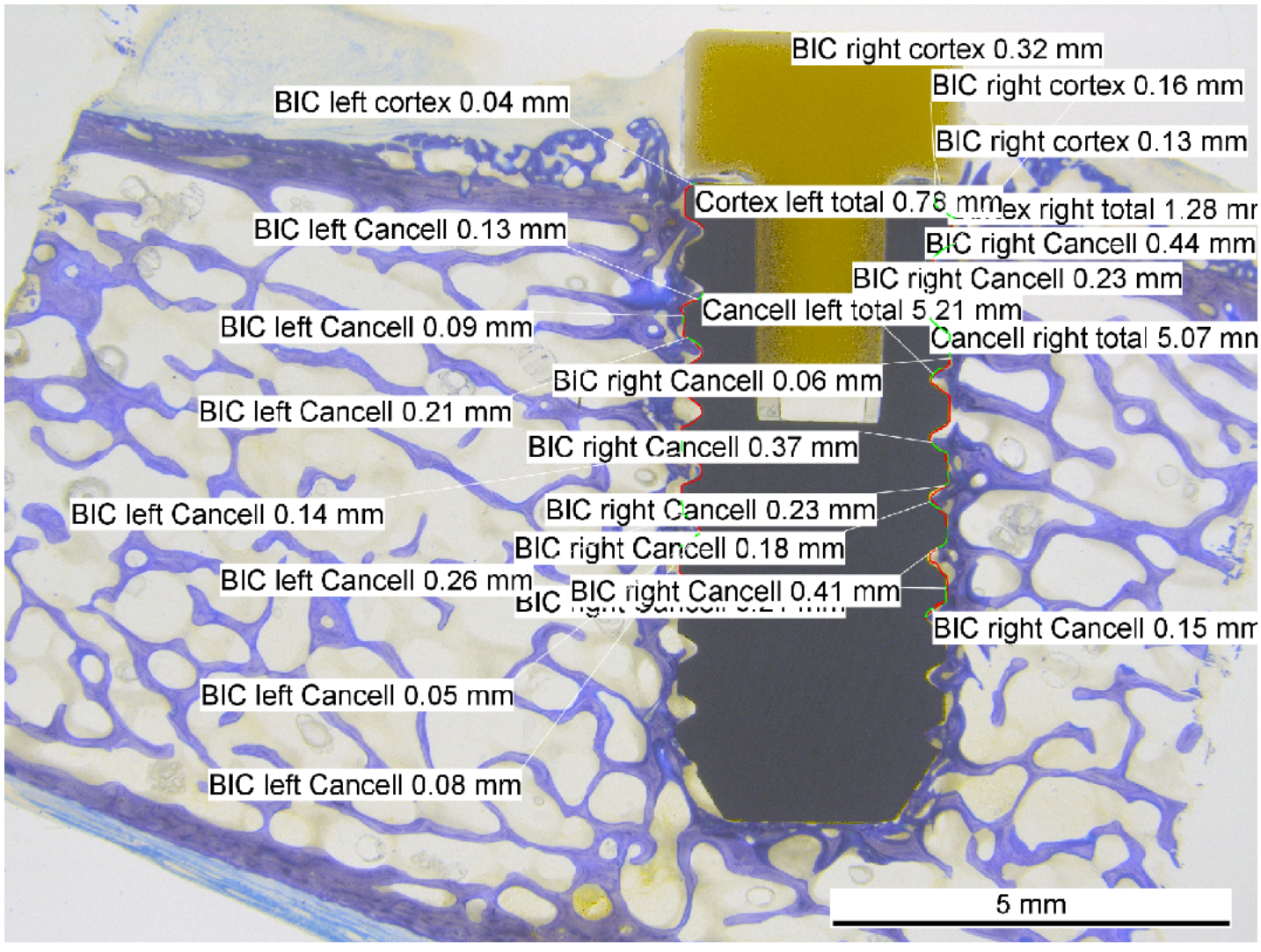

Fig.3: Evaluation of the BIC of a titanium implant. The red lines along the implant surface represent the areas of the implant surface with no bone contact, whereas the green lines represent direct contact areas to the surrounding bone.

STATISTICS

For the graphical illustration of the results the commercial software Origin-Pro 7.5G SR2 (OriginLab Corporation, Northampton, MA, USA) was used.

Statistical analysis was carried out with the commercial software SPSS (SPSS Statistics 20, Mac OS X, Version 13.0, Chicago, IL, USA). One-way factorial analysis of variance (ANOVA) was used to assess overall differences between groups, followed by Bonferroni post hoc comparisons to evaluate differences between individual groups. A significance level was set at $P<0.05$.

RESULTS

SURGERY AND POSTOPERATIVE PERIOD

Surgery and anaesthesia were uneventful. All three sheep showed normal food and water intake 2 days postoperatively. After harvesting the samples, no implant exhibited clinical instability. Ventro-dorsal and latero-lateral radiographs demonstrated that all implants were correctly in place and there were no signs of inflammation, osteolysis or fracture lines.

HISTOLOGICAL EVALUATION AND BIC

Basically, the thickness of the cortical bone decreased from position 1 to 6. At position 6 and partly also at position 5, it was difficult to distinguish a cortical bone from cancellous bone, since the cortex was thinnest there.

All implant groups showed more or less newly formed extraossary woven bone tissue around the sealing caps. Also around the bone-implant interface all implants showed newly formed woven bone, although this was somewhat more pronounced in the presence of a broad cortical bone. In Fig.4 are representative histological images of the thick sections presented. In the area of the threads, especially in the cortical region, newly formed woven bone was visible, which seemed to fill the threads on the MBTv, RGD and KRSR modified implants slightly more than on the titanium and HA-PEEK implants. In the presence of a wide cortical bone, the KRSR and HA-PEEK implants still showed direct contact between the outer flanks of the threads and the old cortical bone. In these areas, the titanium implants generally showed contact with newly formed woven bone that was located between the old cortical bone and the implant surface, whereas the RGD and MBTv implants showed in principle direct contact of the outer flanks of the threads with the old cortical bone (Fig.5). There were also resorption lacunae predominantly visible in the area of the cortical bone around the implants, which were most pronounced on the titanium, HA-PEEK and KRSR implants, so that the original implant bed could no longer be clearly defined by the old cortical bone (Fig.4 and 6).

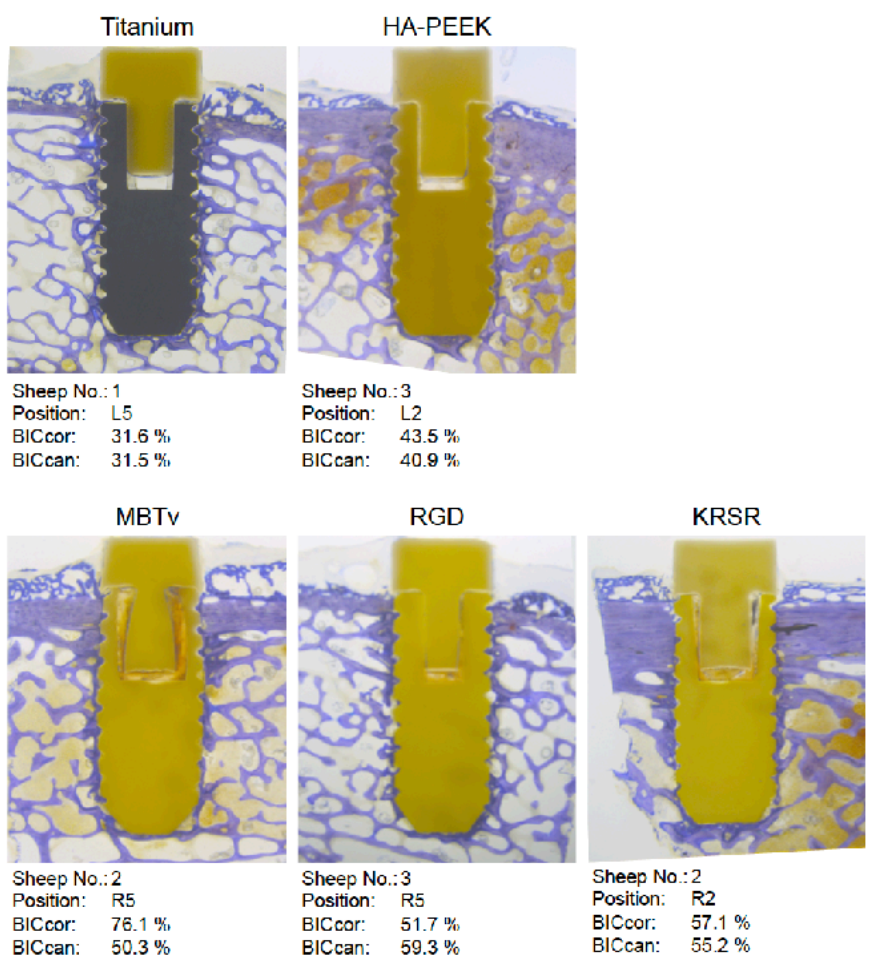

Fig.4: Representative histological images with the BIC values within the cortical (BICcor) and cancellous bone (BICcan). Old bone areas are stained lighter blue and the darker blue bone areas, predominantly in the areas closer to the implants and in the implant threads, represent newly formed bone. For the titanium implant, the BIC is limited to contact with newly formed bone.

Fig.5: Histological images of a MBTv- and a RGD-implant with direct contact to old bone within a wide cortical bone with the BIC values within the cortical (BICcor) and cancellous bone (BICcan). The outer flanks of the threads are in direct contact with the old cortical bone, while the implant threads are mostly filled with newly formed bone.

MBTv

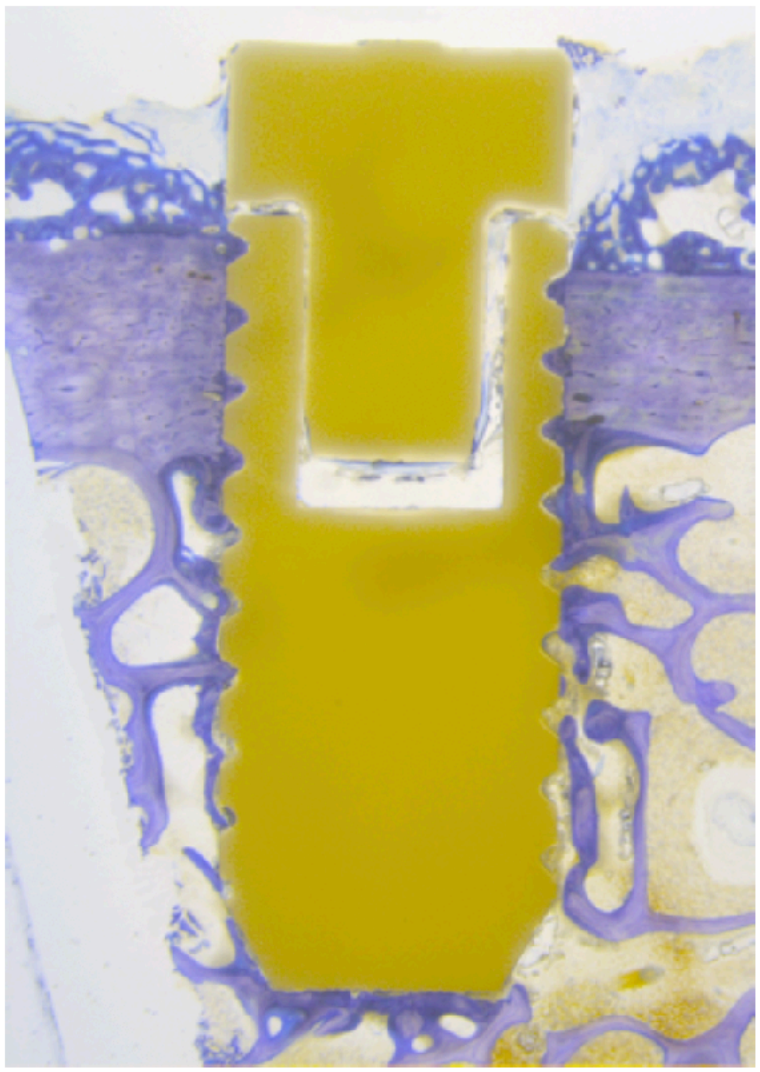

Sheep No.: 1
Position: L1
BICcor: 100 %
BICcan: 55 %

RGD

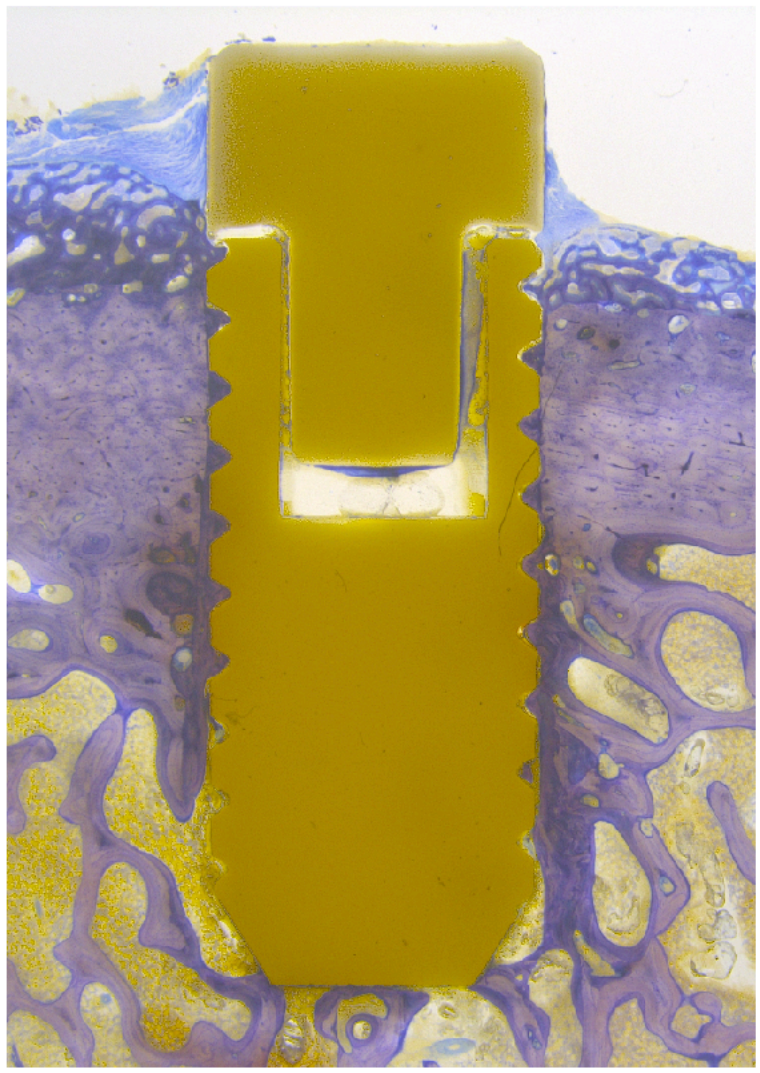

Sheep No.: 2
Position: L1
BICcor: 100 %
BICcan: 63.6 %

KRSR

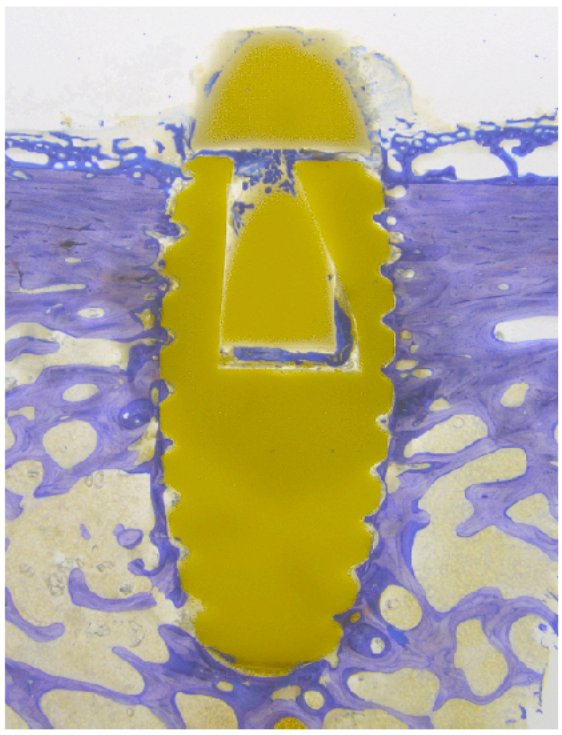

Sheep No.: 2
Position: L2
BICcor: 45.38 %
BICcan: 47 %

Fig.6: Histological image of a KRSR-implant showing pronounced bone remodeling with the BIC values within the cortical (BICcor) and cancellous bone (BICcan). Especially in the cortical area pronounced bone remodeling with is visible.

HISTOMORPHOMETRY

The results of new bone and old bone formation and the BIC are summarized in Table 1.

The results for the area shares of old and newly formed bone in the area of twice the thread depth around the implants are shown in Fig.7 and 8.

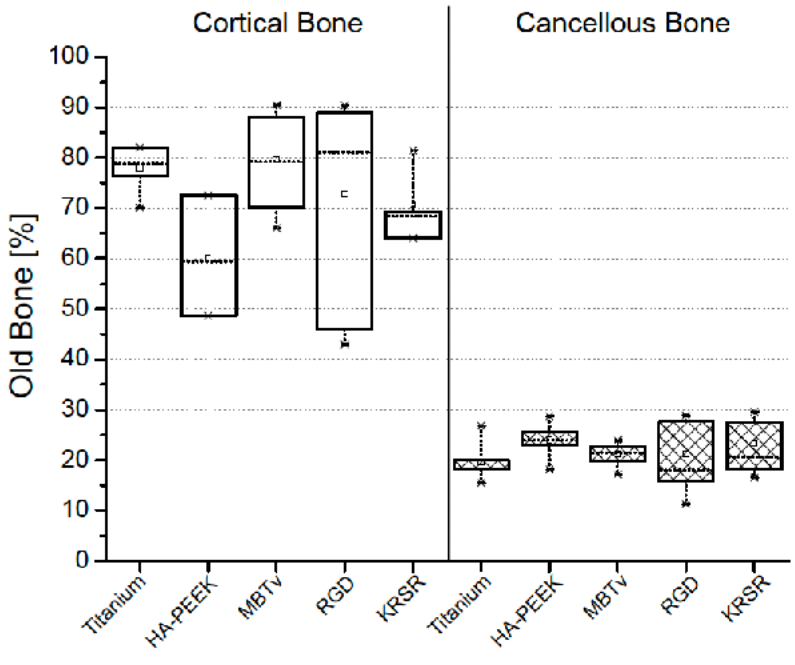

Fig.7: Box plots of the area shares of old bone.

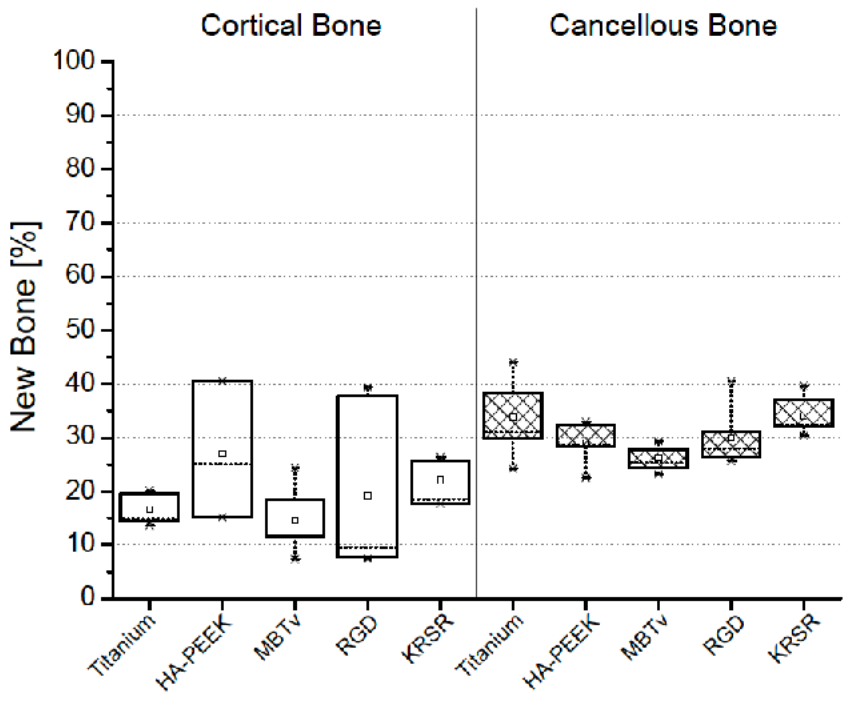

Fig.8: Box plots of the area shares of new bone.

The area percentages of old bone did not differ significantly, with MBTv implants showing the highest percentage of old bone in cortical bone at 79.7 ± 9.8% and HA-PEEK implants showing the lowest percentage of old bone at 60.2 ± 12%. In the area of cancellous bone, the HA-PEEK implants showed the highest proportion of old bone and the titanium implants the lowest (HA-PEEK implants: 24 ± 3.5 %; titanium implants: 19.6 ± 3.9 %).

There were also no significant differences between the groups with regard to the proportion of newly formed bone. In the cortical bone region, HA-PEEK implants showed the highest percentage of newly formed bone with 26.9 ± 12.8 % and MBTv implants the lowest percentage of newly formed bone with 14.6 ± 6 %. These implants also showed the lowest proportion of new bone in the cancellous bone area with 26.1 ± 2.2 %, with the KRSR implants showing the highest proportion of new bone in this area with 34.1 ± 3.5 %.

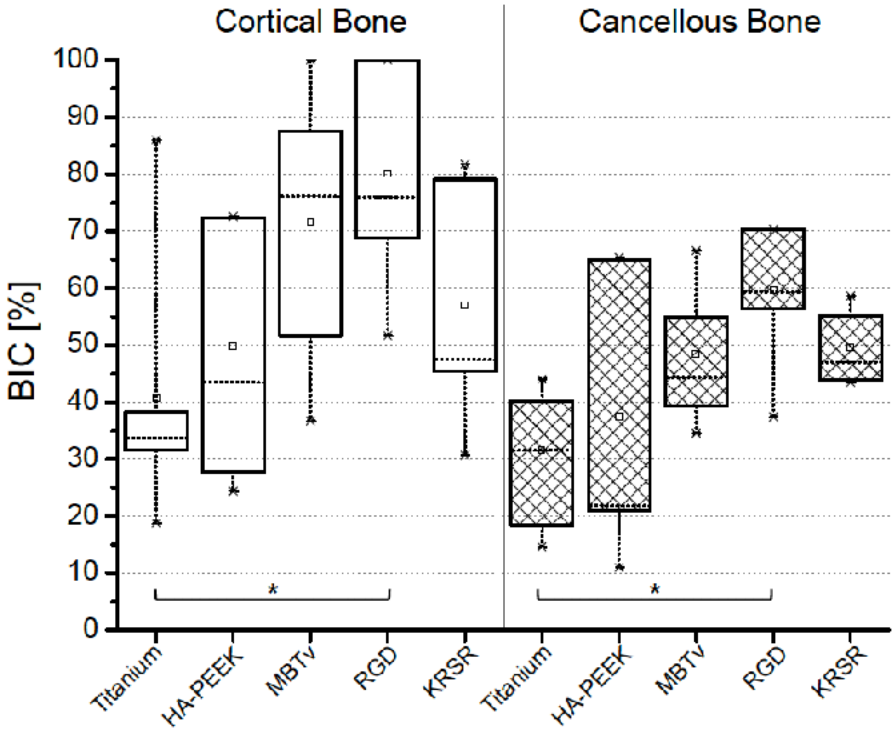

After 8 weeks, the titanium implants showed the lowest average BIC in both cortical and cancellous bone (cortical bone: 40.7 ± 23.2 %; cancellous bone: 31.5 ± 12.3 %). These values differed significantly from the BIC values of the RGD group, which showed approximately twice as high BIC values in both bone regions and the highest BIC values overall (cortical bone: 80 ± 18.8 %; cancellous bone: 59.6 ± 12.2 %; Fig.9).

Fig.9: Box plots of the BIC-values of the different groups (*significant difference between the titanium- and the RGD-implants).

FLUORESCENCE LABELING

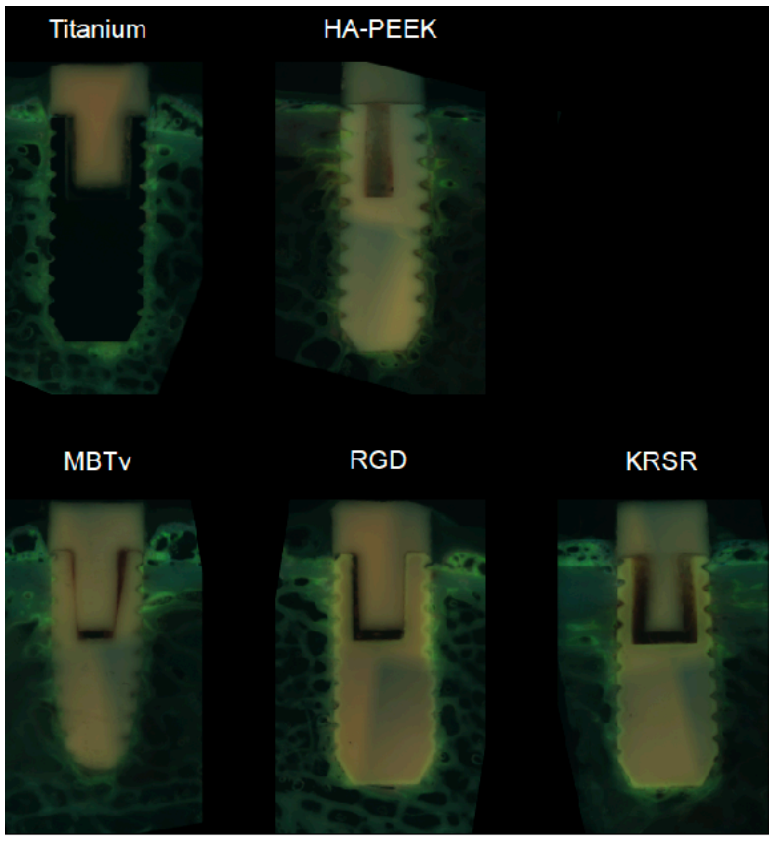

Based on the fluorescence calcein green staining, the highest bone formation could be shown at two weeks postoperatively, which took place in the area of the bone-implant interface and extraossary around the sealing caps of the implants (Fig. 10). On the basis of the fluorescent markings the bone apposition in the area of the threads could be reconstructed (Fig.11), whereby in the area of the bone-implant interface of the titanium implants the proportion of newly formed, oxyteracycline-stained (blue) bone tissue seemed to be somewhat larger compared to the other implants after 8 weeks of healing. In addition, the extraosseous bone in particular showed proportions of blue fluorescent tissue, which indicated bone apposition at this time.

Fig.10: Fluorescence images of the same samples like Fig.5. Due to the calcein green stained areas, the highest rate of bone formation could be observed after 2 weeks around the implants. Afterwards bone was formed towards the implant surface and in the areas of the threads after 4 weeks (xylenol orange) and 8 weeks (oxytetracyclin (blue)). Additionally, due to the oxytetracyclin staining new extraossary bone seemed to be predominantly formed after 8 weeks. Also new bone formation at the implant-bone interface of the titanium implant seemed to be more pronounced after 8 weeks compared to the other groups.

Fig.11: Close-ups of the images of Fig.11. Due to the stained areas after 2 (green), 4 (orange) and 8 weeks (blue) the pattern of bone apposition can be traced back.

DISCUSSION

After a healing period of 8 weeks in the pelvic bone of sheep, all PEEK-based implants showed on average a higher BIC value than the titanium implants of the control group. Since titanium is still considered the gold standard for implant materials, sufficient osseointegration of the PEEK-based implants can be assumed.

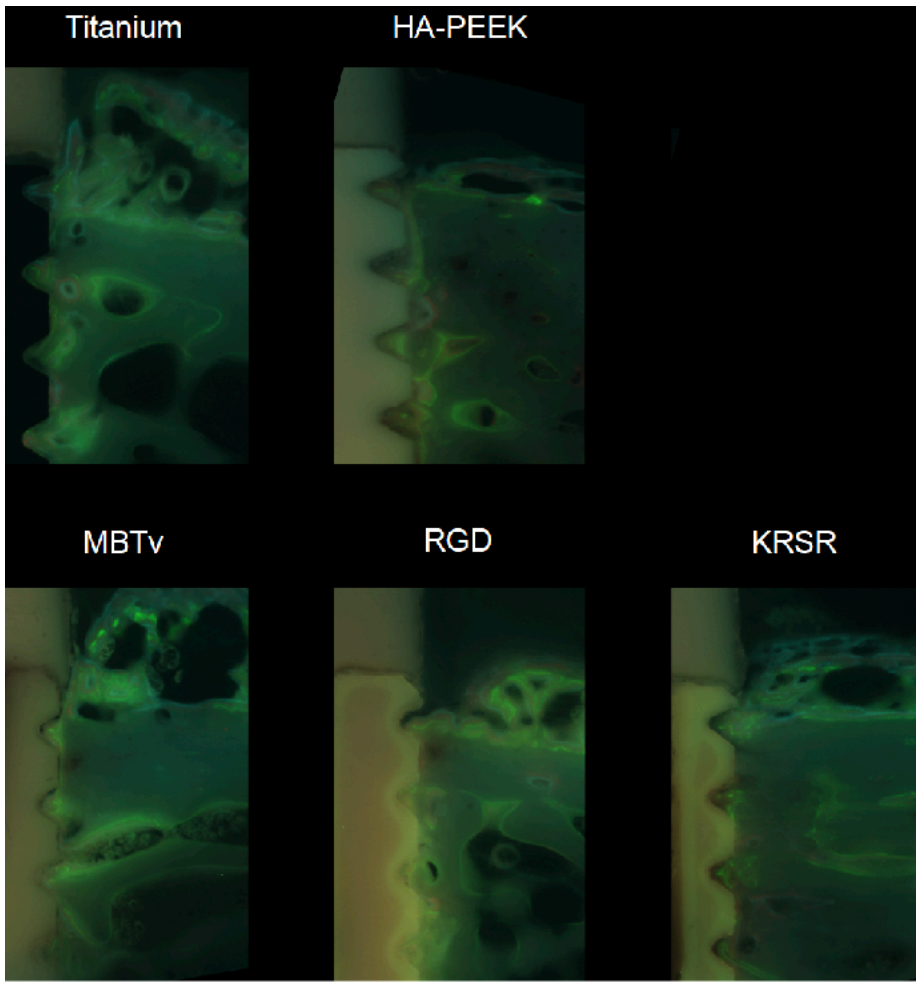

In the present study, only machined implants were used in order to be able to assess only the chemical influence of the surfaces on osseointegration, as rough implant surfaces generally have a significantly positive effect on osseointegration.

Therefore, titanium implants with a sandblasted and acid-etched surface generally showed a BIC value above 50% after 8 weeks of healing in the same animal model (approx. 80% [47]; 57.64 ± 14.12 % [48]; 53.3 ± 9 % [50]). The results of the BIC of the machined titanium implants in the present study seem valid as a reference, since such implants showed comparable values after 8 weeks of implantation in other studies using the same animal model (36.5 ± 23.5 % [51]; 51.7 ± 6.2 % in cortical bone and 27.2 ± 4 % in cancellous bone [52]).

In comparison of the PEEK-based implants, implants with surface modifications showed higher BIC values on average than HA-PEEK implants, while the BIC values of RGD implants in cortical and cancellous bone were significantly higher than those of titanium implants. Such surface modifications in the nanometer range have the advantage that they do not affect the properties of the bulk material, whereas compounding the PEEK matrix with HA particles makes PEEK more brittle [53]. This is because the elastic modulus increases with the degree of filling of HA particles due to the elastic modulus of HA (85 GPa) and the tensile strength decreases [54]. In this respect, Ma et al. considered a filling level of 30% HA in the PEEK matrix to be ideal [54], whereby only the particles on the surface have an influence on osseointegration and the particles in the inner area can detach from the PEEK matrix under load, which leads to a weakening of the composite [53]. In this respect, the material is only suitable for processing by machining, since it cannot be guaranteed that a sufficient number of HA particles will be freely available on the implant surface, for example, when processing by injection molding.

The HA-filled PEEK compound in this study had an HA content of 20 %. In the cortical bone area in particular, a relatively wide range of BIC values was found in comparison with the other implant groups. This could possibly be attributed to an uneven distribution of the HA particles within the matrix and thus on the implant surfaces.
One limitation of the present study was that no untreated PEEK implants were included as negative controls. This was omitted because pure PEEK is generally considered to be poorly osseointegrative [32]. In a study in the literature using the same sheep model, pure PEEK cylinders showed a BIC value of 65 ± 48 % in cortical bone and 34 ± 8 % in cancellous bone after 2 weeks [55]. These values increased to 78 ± 27 % and 66 ± 9 % respectively after 12 weeks [55]. However, these results can be compared to a very limited extent because the implants had a cylindrical shape without thread and therefore sat completely gap-free in the bony implant site, i.e. significantly less newly formed bone was required for the BIC. Furthermore, the healing periods are not comparable, since it must be assumed that new bone formation also takes place beyond a healing period of 8 weeks. For example, cylindrical PEEK implants implanted in the tibia and femur of sheep showed increasing BIC values over a period of 26 weeks (28.4 % after 6 weeks; 41.7 % after 12 weeks; 53.8 % after 26 weeks) [56]. In another sheep model, machined PEEK cylinders showed a similar pattern for the BIC in cortical bone of the tibial diaphysis (≈ 38% at 4 weeks; ≈ 45% at 12 weeks; ≈ 55% at 26 weeks), with the BIC in cancellous bone of the proximal tibia initially increasing from ≈ 22% at 4 weeks to ≈ 29% at 12 weeks and decreasing slightly to ≈ 25% at 26 weeks [35].

An increase in the BIC over a longer period of time can also be assumed for the machined titanium implants of the present study. In the above-mentioned study by von Salis-Soglio et al., the machined titanium implants showed a BIC value of 48.6 ± 5.4 % after 52 weeks, as was the case at least in cancellous bone, which was higher than after healing periods of 2 (36 ± 4.8 %) and 8 weeks (27.2 ± 4 %) [52]. In any case, these implants in cortical bone showed an opposite trend with respect to the BIC, so that it fell from 67.3 ± 8.2 % after 2 weeks, via 51.7 ± 6.2 % after 8 weeks to 42.3 ± 3.7 % after 52 weeks [52].

The blue bone areas stained with oxytetracycline, which were more or less pronounced in the area of the bone-implant interfaces at the end of the present study after 8 weeks, indicate that the bone remodeling was not yet completed. Based on the example of the titanium implant in Fig.11, where these areas appeared somewhat more pronounced compared with the other implant groups, it can be concluded that the BIC would have increased further at this one. Conversely, it could be assumed that the bone remodeling or formation of the experimental PEEK implants was probably largely completed at the end of the present study period. In combination with the higher BIC values of the experimental PEEK implants, it can be concluded that they were osseointegrated by earlier bone formation [57].

In an animal experiment with New Zealand rabbits, the positive influence of an RGD coating on osseointegration was demonstrated [41]. After 3 weeks RGD-coated titanium implants showed a significantly higher BIC value compared to unmodified titanium implants (63 ± 2.4 % vs. 49 ± 5.5 %).

In a study with miniature pigs, no influence of a titanium implant coating with KRSR peptide (BIC: 38.45 ± 22.62 %) or a combination of KRSR and RGD peptides in two different concentrations (20 pmol/cm^2 KRSR/0.05 pmol/cm^2 RGD, BIC: 35.22 ± 22.57 %; 20 pmol/cm^2 KRSR/1.26 pmol/cm^2, BIC: 35.61 ± 15.12 %) on osseointegration could be demonstrated in comparison to unmodified titanium implants (BIC: 41.49 ± 27.43 %) [58]. The implants

with KRSR peptide coating showed a slightly lower proportion of new bone in comparison with unmodified implants (28.58 ± 9.94 % vs. 30.61 ± 7.11 %).

After implant placement, a certain amount of bone resorption generally occurs initially as response to surgery, which is accompanied by a drop in the implant stability quotient (ISQ) in the period from the first to the third and fourth week [57], whereby the formation of new bone causes secondary implant stability via osseointegration [59].
In this respect the lowest possible resorption of the old local bone is desirable, not least because bone resorption also occurs due to foreign body reactions [60]. At the same time, as little new bone as possible should be formed in the course of osseointegration, since otherwise sclerosing tends to occur, which may be later associated with implant loss [61]. At the same time, the titanium implants in this study showed that much newly formed bone cannot be equated with a high BIC.

In this respect it can be assumed that the characteristics of the ideal osseointegration of an implant is based on the (a) highest possible BIC value in combination with the (b) highest possible proportion of old bone and the (c) lowest possible proportion of new bone, which would put titanium as the ideal implant material in a different light. In this respect, the coating with KRSR peptide may also have to be assessed critically against this background due to the pronounced bone remodeling as shown in Fig.6.

MBTv implants however showed an (a) overall high BIC in combination with the (b) highest proportion of old cortical bone and the (c) lowest proportion of newly formed bone and therefore met the three characteristics of stable osseointegration.

Compared to titanium as conventional evidence-based implant material in general, theoretically all tested implant types could be used. For RGD and KRSR, this would have to be verified in the future by long-term results of in-vivo studies also under mechanical loading of the implants.

CONCLUSION

Compared to titanium as the gold standard of implant materials, all PEEK-based implant types appeared promising with regard to osseointegration. Surface-modified PEEK implants should possibly be preferred over HA-filled PEEK compounds, since corresponding PEEK implants can also be manufactured by injection molding, for example, and the surface modification does not impair the mechanical properties of the bulk material.

REFERENCES

[1] Brånemark PI, Adell R, Breine U, Hansson BO, Lindström J, Ohlsson A. Intraosseous anchorage of dental prostheses. I. Experimental studies. Scand J Plast Reconstr Surg. 1969;3(2):81-100.

[2] Pessôa de Oliveira PGF, Bergamo ETP, Neiva R, Bonfante EA, Witek L, Tovar N, Coelho PG. Osseodensification outperforms conventional implant subtractive instrumentation: A study in sheep. Mater Sci Ing C. 2018;90:300-307.

[3] Adell R, Lekholm U, Rockler B, Branemark PI. A 15-year study of osseointegrated implants in the treatment of the edentulous jaw, Int. J. Oral Surg. 1981;10:387-416.

[4] Wheelis SE, Montaño-Figueroa AG, Quevedo-Lopez M, Rodrigues DC. Effects of titanium oxide surface properties on bone-forming and soft tissue-forming cells. Clin Implant Dent Relat Res. 2018;20(5): 838-847.

[5] De Tullio I, Berardini M, Di Iorio D, Perfetti F, Perfetti G. Comparative evaluation among laser-treated, machined, and sandblasted/acid-etched implant surfaces: an in vivo histologic analysis on sheep. Int J Implant Dent. 2020;6(1):7.

[6] Furiya-Sato S, Fukushima A, Mayanagi G, Sasaki K, Takahashi N. Electrochemical evaluation of the hydrogen peroxide- and fluoride-induced corrosive property and its recovery on the titanium surface. J Prosthodont Res. 2019 Oct 16. pii: S1883-1958(19)30042-8.

[7] Eliaz N. Corrosion of Metallic Biomaterials: A Review. Materials (Basel). 2019;12(3). pii: E407.

[8] Berbel LO, Banczek EDP, Karoussis IK, Kotsakis GA, Costa I. Determinants of corrosion resistance of Ti-6Al-4V alloy dental implants in an In Vitro model of peri-implant inflammation. PLoS One. 2019;14(1):e0210530.

[9] Alrabeah GO, Knowles JC, Petridis H. Reduction of Tribocorrosion Products When Using the Platform-Switching Concept. J Dent Res. 2018;97(9):995-1002.

[10] Dörner T, Haas J, Loddenkemper C, von Baehr V, Salama A. Implant-related inflammatory arthritis. Nat Clin Pract Rheumatol. 2006 Jan;2(1):53-6; quiz 57.

[11] Jacobi-Gresser E, Huesker K, Schütt S. Genetic and immunological markers predict titanium implant failure: a retrospective study. Int J Oral Maxillofac Surg. 2013;42(4):537-43.

[12] Takahashi K, Shiraishi N, Ishiko-Uzuka R, Anada T, Suzuki O, Masumoto H, Sasaki K. Biomechanical evaluation of Ti-Nb-Sn alloy implants with a low Young's modulus. Int J Mol Sci. 2015;16(3):5779-88.

[13] Skalak R. Biomechanical considerations in osseointegrated prostheses. J Prosthet Dent. 1983;49(6):843-8.

[14] Soumeire J, Dejou J. Shock absorbability of various restorative materials used on implants. J Oral Rehabil. 1999;26(5):394-401.

[15] Quirynen M, Naert I, van Steenberghe D. Fixture design and overload influence marginal bone loss and fixture success in the Brånemark system. Clin Oral Implants Res. 1992 Sep;3(3):104-11.

[16] Isidor F. Loss of osseointegration caused by occlusal load of oral implants. A clinical and radiographic study in monkeys. Clin Oral Implants Res. 1996 Jun;7(2):143-52.

[17] Brunski JB. In vivo bone response to biomechanical loading at the bone/dental-implant interface. Adv Dent Res. 1999 Jun;13:99-119.

[18] Nagasawa M, Takano R, Maeda T, Uoshima K. Observation of the bone surrounding an overloaded implant in a novel rat model. Int J Oral Maxillofac Implants. 2013 Jan-Feb;28(1):109-16.

[19] Kettunen J, Kröger H, Bowditch M, Joukainen J, Suomalainen O. Bone mineral density after removal of rigid plates from forearm fractures: preliminary report. J Orthop Sci. 2003;8(6):772-6.

[20] Kim YH, Park JW, Kim JS. Ultrashort versus Conventional Anatomic Cementless Femoral Stems in the Same Patients Younger Than 55 Years. Clin Orthop Relat Res. 2016;474(9):2008-17.

[21] Andreiotelli M, Wenz HJ, Kohal RJ. Are ceramic implants a viable alternative to titanium implants? A systematic literature review. Clin Oral Implants Res. 2009;20 Suppl 4:32-47.

[22] Cionca N, Hashim D, Mombelli A. Zirconia dental implants: where are we now, and where are we heading? Periodontol 2000. 2017;73(1):241-258.

[23] Haro Adánez M, Nishihara H, Att W. A systematic review and meta-analysis on the clinical outcome of zirconia implant-restoration complex. J Prosthodont Res. 2018 Jul 5. pii: S1883-1958(18)30082-3.

[24] Parmigiani-Izquierdo JM, Cabaña-Muñoz ME, Merino JJ, Sánchez-Pérez A. Zirconia implants and peek restorations for the replacement of upper molars. Int J Implant Dent. 2017;3(1):5.

[25] Kurtz SM, Devine JN. PEEK biomaterials in trauma, orthopedic, and spinal implants. Biomaterials. 2007;28(32):4845-69.

[26] Schwitalla AD, Spintig T, Kallage I, Müller WD. Pressure behavior of different PEEK materials for dental implants. J Mech Behav Biomed Mater. 2016;54:295-304.

[27] Hasegawa T, Ushirozako H, Shigeto E, Ohba T, Oba H, Mukaiyama K, Shimizu S, Yamato Y, Ide K, Shibata Y, Ojima T, Takahashi J, Haro H, Matsuyama Y. The Titanium-Coated PEEK Cage Maintains Better Bone Fusion with the Endplate than the PEEK Cage 6 Months After PLIF Surgery-A Multicenter, Prospective, Randomized Study. Spine (Phila Pa 1976). 2020 Mar 6.

[28] Koh YG, Park KM, Lee JA, Nam JH, Lee HY, Kang KT. Total knee arthroplasty application of polyetheretherketone and carbon-fiber-reinforced polyetheretherketone: A review. Mater Sci Eng C Mater Biol Appl. 2019 ;100:70-81.

[29] Allemann F, Halvachizadeh S, Rauer T, Pape HC. Clinical outcomes after carbon-plate osteosynthesis in patients with distal radius fractures. Patient Saf Surg. 2019;13:30.

[30] Alibhai MK, Balasundaram I, Bridle C, Holmes SB. Is there a therapeutic role for cranioplasty? Int J Oral Maxillofac Surg 2013;42:559-61.

[31] Jiang X, Yao Y, Tang W, Han D, Zhang L, Zhao K, Wang S, Meng Y. Design of Dental Implants at Materials Level: An Overview. J Biomed Mater Res A. 2020 Mar 20. doi: 10.1002/jbm.a.36931. [Epub ahead of print] Review.

[32] Briem D, Strametz S, Schröder K, Meenen NM, Lehmann W, Linhart W, Ohl A, Rueger JM. Response of primary fibroblasts and osteoblasts to plasma treated polyetheretherketone (PEEK) surfaces. J Mater Sci Mater Med. 2005;16(7):671-7.

[33] Makino T, Kaito T, Sakai Y, Takenaka S, Yoshikawa H. Computed tomography color mapping for evaluation of bone ongrowth on the surface of a titanium-coated polyetheretherketone cage in vivo: A pilot study. Medicine (Baltimore). 2018;97(37):e12379.

[34] Barkarmo S, Andersson M, Currie F, Kjellin P, Jimbo R, Johansson CB, Stenport V. Enhanced bone healing around nanohydroxyapatite-coated polyetheretherketone implants: An experimental study in rabbit bone. J Biomater Appl. 2014;29(5):737-47.

[35] Poulsson AH, Eglin D, Zeiter S, Camenisch K, Sprecher C, Agarwal Y, Nehrbass D, Wilson J, Richards RG. Osseointegration of machined, injection moulded and oxygen plasma modified PEEK implants in a sheep model. Biomaterials. 2014 Apr;35(12):3717-28.

[36] Ma R, Yu Z, Tang S, Pan Y, Wei J, Tang T. Osseointegration of nanohydroxyapatite- or nano-calcium silicate-incorporated polyetheretherketone bioactive composites in vivo. Int J Nanomedicine. 2016 Nov 14;11:6023-6033.

[37] Walsh WR, Pelletier MH, Bertollo N, Christou C, Tan C. Does PEEK/HA Enhance Bone Formation Compared With PEEK in a Sheep Cervical Fusion Model? Clin Orthop Relat Res. 2016;474(11):2364-2372.

[38] Bell BF, Schuler M, Tosatti S, Textor M, Schwartz Z, Boyan BD. Osteoblast response to titanium surfaces functionalized with extracellular matrix peptide biomimetics. Clin Oral Implants Res. 2011;22(8):865-72.

[39] Staines KA, MacRae VE, Farquharson C. The importance of the SIBLING family of proteins on skeletal mineralisation and bone remodelling. J Endocrinol 2012;214:241-255.

[40] Chen Q, Shou P, Zhang L, Xu C, Zheng C, Han Y, Li W, Huang Y, Zhang X, Shao C, Roberts AI, Rabson AB, Ren G, Zhang Y, Wang Y, Denhardt DT, Shi Y. An osteopontin-integrin interaction plays a critical role in directing adipogenesis and osteogenesis by mesenchymal stem cells. Stem Cells. 2014;32(2):327-37.

[41] Heller M, Kumar VV, Pabst A, Brieger J, Al-Nawas B, Kämmerer PW. Osseous response on linear and cyclic RGD-peptides immobilized on titanium surfaces in vitro and in vivo. J Biomed Mater Res A. 2018;106(2): 419-427.

[42] Wang H, Li Q, Wang Q, Zhang H, Shi W, Gan H, Song H, Wang Z. Enhanced repair of segmental bone defects in rabbit radius by porous tantalum scaffolds modified with the RGD peptide. J Mater Sci Mater Med. 2017;28(3):50.

[43] Zhu Y, Cao Z, Peng Y, Hu L, Guney T, Tang B. Facile Surface Modification Method for Synergistically Enhancing the Biocompatibility and Bioactivity of Poly(ether ether ketone) That Induced Osteodifferentiation. ACS Appl Mater Interfaces. 2019;11(31):27503-27511.

[44] Becker M, Lorenz S, Strand D, Vahl CF, Gabriel M. Covalent grafting of the RGD-peptide onto polyetheretherketone surfaces via Schiff base formation. ScientificWorldJournal. 2013 Oct 21;2013:616535.

[45] Hoyos-Nogués M, Falgueras-Batlle E, Ginebra MP, Manero JM, Gil J, Mas-Moruno C. A Dual Molecular Biointerface Combining RGD and KRSR Sequences Improves Osteoblastic Functions by Synergizing Integrin and Cell-Membrane Proteoglycan Binding. Int J Mol Sci. 2019;20(6).

[46] Knaus J, Schaffarczyk D, Cölfen H. On the Future Design of Bio-Inspired Polyetheretherketone Dental Implants. Macromol Biosci. 2020;20(1):e1900239.

[47] Langhoff JD, Voelter K, Scharnweber D, Schnabelrauch M, Schlottig F, Hefti T, Kalchofner K, Nuss K, von Rechenberg B. Comparison of chemically and pharmaceutically modified titanium and zirconia implant surfaces in dentistry: a study in sheep. Int J Oral Maxillofac Surg. 2008;37(12):1125-32.

[48] Stübinger S, Biermeier K, Bächi B, Ferguson SJ, Sader R, von Rechenberg B. Comparison of Er:YAG laser, piezoelectric, and drill osteotomy for dental implant site preparation: a biomechanical and histological analysis in sheep. Lasers Surg Med. 2010;42(7):652-61.

[49] von Rechenberg B, Guenther H, McIlwraith CW, Leutenegger C, Frisbie DD, Akens MK, Auer JA. Fibrous tissue of subchondral cystic lesions in horses produce local mediators and neutral metalloproteinases and cause bone resorption in vitro. Vet Surg. 2000 Sep-Oct;29(5):420-9.

[50] Stübinger S, Nuss K, Bürki A, Mosch I, le Sidler M, Meikle ST, von Rechenberg B, Santin M. Osseointegration of titanium implants functionalised with phosphoserine-tethered poly(epsilon-lysine) dendrons: a comparative study with traditional surface treatments in sheep. J Mater Sci Mater Med. 2015;26(2):87.

[51] Plecko M, Sievert C, Andermatt D, Frigg R, Kronen P, Klein K, Stübinger S, Nuss K, Bürki A, Ferguson S, Stoeckle U, von Rechenberg B. Osseointegration and biocompatibility of different metal implants--a comparative experimental investigation in sheep. BMC Musculoskelet Disord. 2012;13:32.

[52] von Salis-Soglio M, Stübinger S, Sidler M, Klein K, Ferguson SJ, Kämpf K, Zlinszky K, Buchini S, Curno R, Péchy P, Aronsson BO, von Rechenberg B. A novel multi-phosphonate surface treatment of titanium dental implants: a study in sheep. J Funct Biomater. 2014;5(3):135-57.

[53] Hughes EA, Parkes A, Williams RL, Jenkins MJ, Grover LM. Formulation of a covalently bonded hydroxyapatite and poly(ether ether ketone) composite. J Tissue Eng. 2018;9:2041731418815570.

[54] Ma R, Guo D. Evaluating the bioactivity of a hydroxyapatite-incorporated polyetheretherketone biocomposite. J Orthop Surg Res. 2019;14(1):32.

[55] Stübinger S, Drechsler A, Bürki A, Klein K, Kronen P, von Rechenberg B. Titanium and hydroxyapatite coating of polyetheretherketone and carbon fiber-reinforced polyetheretherketone: A pilot study in sheep. J Biomed Mater Res B Appl Biomater. 2016;104(6):1182-91.

[56] Meers CM, Verleye GB, Smeets D, Van Hauwermeiren HY, Loeckx D, Willems K, Siau VG, Lauweryns PJ. Fine grained osseointegrative coating improves biocompatibility of PEEK in heterotopic sheep model. Int J Spine Surg. 2015;9:35.

[57] Mangano C, Shibli JA, Pires JT, Luongo G, Piattelli A, Iezzi G. Early Bone Formation around Immediately Loaded Transitional Implants Inserted in the Human Posterior Maxilla: The Effects of Fixture Design and Surface. Biomed Res Int. 2017;2017:4152506.

[58] Broggini N, Tosatti S, Ferguson SJ, Schuler M, Textor M, Bornstein MM, Bosshardt DD, Buser D. Evaluation of chemically modified SLA implants (modSLA) biofunctionalized with integrin (RGD)- and heparin (KRSR)-binding peptides. J Biomed Mater Res A. 2012;100(3):703-11.

[59] Bernhardt R, Kuhlisch E, Schulz MC, Eckelt U, Stadlinger B. Comparison of bone-implant contact and bone-implant volume between 2D-histological sections and 3D-SRμCT slices. Eur Cell Mater. 2012;23:237-47; discussion 247-8.

[60] Mattila S, Haapamäki V, Waris E. Unfavourable early outcomes of total trapeziectomy with RegJoint™ interposition: a report of 38 osteoarthritic hands in 34 patients. J Hand Surg Eur Vol. 2020;45(2):167-172.

[61] Miyamoto I, Takahashi T, Tanaka T, Hirayama B, Tanaka K, Yamazaki T, Morimoto Y, Yoshioka I. Dense cancellous bone as evidenced by a high HU value is predictive of late implant failure: a preliminary study. Oral Radiol. 2018;34(3):199-207.

You need no coating,

all you need is MBT.

Mimicking Bone Technology

A Golden Standard Technology